Regime Transitions in a Nonreptating Polymer: Cross-Linked Linear Polyethylene

P. J. Phillips* and W. S. Lambert

Department of Materials Science and Engineering, University of Tennessee, Knoxville, Tennessee 37996-2200. *Received August 1, 1989; Revised Manuscript Received September 26, 1989*

ABSTRACT: The bulk crystallization kinetics of linear polyethylene, cross-linked to various levels using Vul-Cup R peroxide, have been determined. The kinetics of the sol fractions of the cross-linked polyethylene conform to regime I growth, while the gel fractions show primarily regime III growth. The regime II–regime III transition can be observed in the gel fractions of high cross-link density over the temperature range 109–113 °C. The behavior is interpreted in terms of the effect of cross-links on the competing rates of surface nucleation and substrate completion. Literal interpretations of Avrami coefficients suggest a disklike morphology that becomes increasingly fibrillar at high levels of cross-link density.

Introduction

Since the concept of a regime transition in polymer crystallization was introduced by Hoffman and Lauritzen in 1973[1] and experimental verification of the regime I–regime II transition identified in polyethylene fractions,[2] there have been several analyses of polymer crystallization in which regime transitions have been identified. The prediction of a third regime followed shortly thereafter,[3,4] and it is now generally recognized that the regime II–regime III transition is quite common.[5] All three regimes have been observed in *cis*-polyisoprene,[6] poly(3,3-dimethylthietane),[7] and, possibly, polypropylene.[8] There may also be a reversion at high temperatures from regime I to regime II in *cis*-polyisoprene[6] and in poly(ethylene oxide).[9]

Although it is now accepted that regimes exist, little attention has been paid to the reasons why they do or do not exist in the polymers that have been studied. Nor has serious consideration been given to how these transitions may be influenced by molecular variables and to how the transition temperatures may be controlled.

In this contribution, a polymer has been considered in which two important molecular variables have been manipulated in a controlled manner through the use of peroxide cross-linking in the molten state. These two variables are (a) the mobility of the polymer chain and (b) the incorporation of noncrystallizable microstructural impurities into the main chain of the polymer. As such, it permits an evaluation of the importance of reptation and copolymerization in the determination of regime transition temperatures.

Regimes can most easily be envisioned as resulting from the relative rates of two competing processes: secondary nucleation and surface spreading. If the rate of deposition of secondary nuclei is i and the rate of surface spreading is g, then when expressed in units of area covered per unit time, the regimes correspond to the following conditions:

regime I	$i \ll g$
regime II	$i \sim g$
regime III	$i > g$

Molecular variables will influence the regime transition temperatures through their effects on these two rates. In the classical theories of crystal growth, $g \gg i$ because of the much lower surface free energy penalty on deposition of a crystallizing unit into a niche than onto a flat surface. Because of this effect, it can be predicted that g will be much more dependent on the mobility of the polymer chain than i. The polymer chain can move into crystallographic register through several possible mechanisms of chain motion.[10–13] One of the most important mechanisms is reptation[14] which was introduced into secondary nucleation theory by Hoffman.[15] Reptation is a specific motion requiring that the chain ends be free, thereby permitting a translation of the center of mass of the chain. In a cross-linked polymer this motion is no longer possible; however, the chains still remain flexible and must use the remaining modes of motion in order to translate. It is to be expected that the elimination of reptation through cross-linking should have a catastropic effect on the value of g, if surface spreading occurs largely through adjacent reentry folding, and that the result should be the production of regime III growth. Such an effect has already been seen in the cross-linking of low-density polyethylene[16] where growth switched from regime II to regime III. The branching frequency in low-density polyethylene vastly exceeds the cross-link frequency even for high cross-link densities, and so only the mobility is affected by molecular changes.

Microstructural impurities that are rejected from the crystal serve as an inpediment to secondary nucleation since a nucleus must contain continuous sections of crystallizable chain. It has already been shown by Andrews et al.[17] that there is an inverse logarithmic relationship between linear growth rate and microstructural impurity levels. It would be expected that the growth rate should change in a similar manner as the cross-link frequency is increased, on the assumption that cross-links are excluded from the crystal. Hence, two opposing influences on regime transition temperatures would be present in cross-linked linear polyethylene. In this paper the influence of cross-link density on regimes and regime transition temperatures will be reported for a linear polyethylene cross-linked in the melt using a peroxide, to ensure uniformity of the network structure.

Experimental Section

The material used was Sclairlink, supplied by Du Pont of Canada, a powdered high-density polyethylene containing the peroxide bis(*tert*-butylperoxyisopropyl)benzene, which is commercially available from Hercules under the trade name Vul-Cup R. Sclairlink was used as the base material following the

0024-9297/90/2223-2075$02.50/0

Table I
Molecular Weight Data of Sol Fractions

sample	M_n	M_w	M_z	M_w/M_n
OPE	12738	42 427	106 111	3.33
S-0.1	7106	20 014	56 521	2.81
S-0.3	7077	22 551	70 319	3.19
S-0.5	6422	16 653	44 949	2.59
S-0.9	4561	8 705	13 471	1.90
S-1.2	4634	11 245	50 294	2.33
S-2.5	4150	14 015	76 318	3.38

Table II
Molecular Weight and Average Chain Length between Cross-Links of Gel Fractions

sample	MW between X-links, $\times 10^{-3}$	av CH_2 units
S-0.1	17.3	1238
S-0.3	12.7	907
S-0.5	5.7	410
S-0.9	3.6	255
S-1.2	3.1	219
S-2.5	1.9	136
S-3.1	1.3	95

removal of the Vul-Cup R from the Sclairlink powder. Materials with different degrees of cross-linking were prepared as described previously.[18,19] Sample preparation and analytical techniques have already been discussed[18,19] and will not be reported here. Specimens were extracted to remove the sol fractions, both sol and gel fractions being studied separately. Characteristics of the specimens are given in Tables I and II. The following nomenclature is used throughout. OPE is original polyethylene, containing no peroxide. S-*n* is extractable or sol fraction from cross-linked sample of *n* wt % peroxide (e.g. S-0.1 is the sol fraction from the 0.1 wt % peroxide sample). G-*n* is the cross-linked extracted or gel fraction produced from *n* loaded polyethylene.

Crystallization kinetics were obtained by using the changes in transmitted light intensity[16,20-22] measured by using a photomultiplier attached to the column of a Reichert-Neovar-Pol polarizing microscope with an attached Mettler hot stage and temperature controller. Samples were held in the melt at 160 °C for 15 min prior to all experiments, before being rapidly quenched to the required crystallization temperature by the inflow of cool nitrogen gas. Crystallization was not observed prior to reaching the required crystallization temperature.

Results

The simplest method of presenting crystallization kinetic data is to plot the reciprocal of the halftime for crystallization versus the crystallization temperature. Such a plot is shown in Figure 1 for the original un-cross-linked polyethylene (OPE) and the sol fractions, where it can be seen that the rate of crystallization decreases rapidly with crystallization temperature for both OPE and the sol fractions. The rate of crystallization of the sol fractions increases with Vul-Cup loading for specimens of 0.1% and 0.3% loading but then decreases as Vul-Cup levels are increased further. This behavior may be a result of the decreasing molecular weight increasing the rate of crystallization at first but then the increasing branch levels causing a decreasing rate for higher Vul-Cup levels. Hoffman and Miller[23] found the growth rate of PE fractions to vary inversely with the square root of the weight-average molecular weight. The molecular weight data of the sol fractions in Table I, when combined with curves of Figure 1, show that such behavior is not followed. This is probably because of differences in branching levels with cross-link density as discussed in the previous reports.[18,19]

The crystallization behavior of the gel fractions may be seen in Figure 2 where it can be seen that increasing Vul-Cup loading results in a continuous decrease in rate,

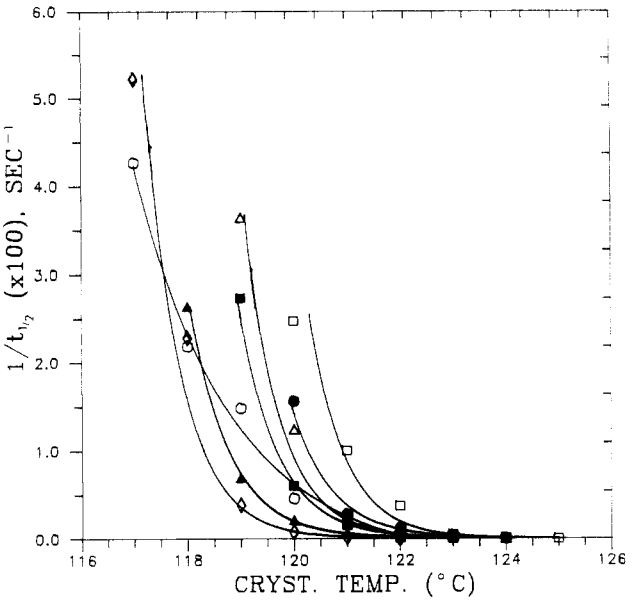

Figure 1. Reciprocal halftimes of sol fractions as a function of crystallization temperature (○, OPE; ●, S-0.1, M_n = 7106; □, S-0.3, M_n = 7077; ■, S-0.5, M_n = 6422; △, S-0.9, M_n = 4561; ▲, S-1.2, M_n = 4634; ◇, S-2.5, M_n = 4150).

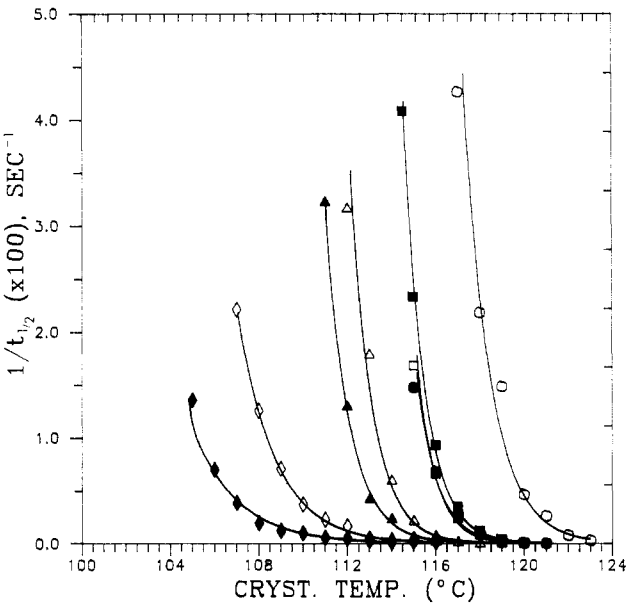

Figure 2. Reciprocal halftimes of gel fractions as a function of crystallization temperature (○, OPE; ●, G-0.1, molecular weight between cross-links (MWX) = 17 300; □, G-0.3, MWX = 12,700; ■, G-0.5, MWX = 5700; △, G-0.9, MWX = 3600; ▲, G-1.2, MWX = 3100; ◇, G-2.5, MWX = 1900; ♦, G-3.1, MWX = 1300).

with the exception that specimens G-0.1, G-0.3, and G-0.5 are virtually indistinguishable fron one another. Specifically, it can be seen that the initial addition of Vul-Cup from OPE to G-0.1 (molecular weight between cross-links of 17 300) reduces the rate of crystallization by a factor of 20 at 117 °C. The crystallization temperature is decreased from 119 (OPE) to 105 °C (G-3.1; molecular weight between cross-links of 1300) for a constant reciprocal halftime.

Discussion

Bulk crystallization rates are not simple to interpret because they do not provide information on the individual contributions of the nucleation rates, growth rates, and secondary crystallization rates involved. However, it is possible to determine the number of regimes exist-

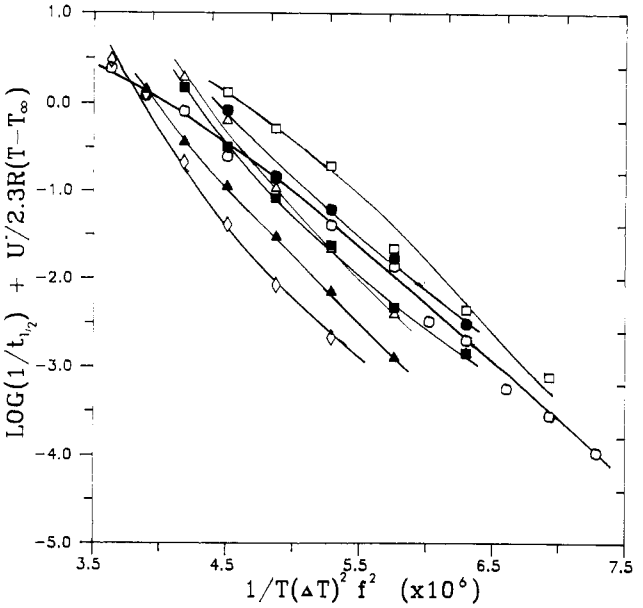

Figure 3. Kinetic behavior of sol fractions assuming homogeneous nucleation (symbols as in Figure 1).

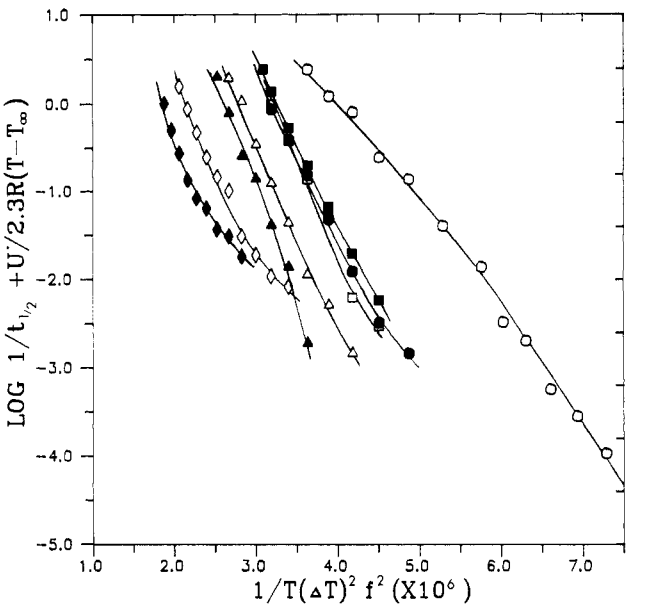

Figure 4. Kinetic behavior of gel fractions assuming homogeneous nucleation (symbols as in Figure 2).

ing over the crystallization temperature range and also the regime transition temperatures.[24] Ross and Frolen[25] have used reciprocal halftime data to give a reasonable indication of crystallization behavior. The approach of Suzuki and Kovacs,[26] which uses U^* to allow for the effect of mobility, has been used here. An assumption of the nucleation type must be made in order to correctly analyze the bulk kinetic data. If heterogeneous nucleation dominates, an inverse dependence on supercooling occurs and the data are a reflection of the linear growth process; however, if homogeneous nucleation dominates, the inverse dependence is on the square of the supercooling. An assumption of homogeneous nucleation leads to the plot

$$\log (t_{1/2}) + U^*/2.3R(T - T_\infty) \text{ versus } 1/T(\Delta T)^2 f^2$$

where f is a factor which corrects for variation in the heat of fusion with temperature below the equilibrium melting point. f was taken as $2T/(T_m^\circ + T)$, with T_m° being 417.7 K.[24,27] Suzuki and Kovacs[26] used $U^* = 1500$ cal mol^{-1} and $T_\infty \sim T_g - 30$ K. The best estimate available for the glass transition temperature of linear polyethylene is 190 K.[28]

Curves result when this analysis is carried out for both the sol and gel fractions meaning that homogeneous nucleation is not of major importance (Figures 3 and 4). Therefore, further analysis is necessary using the assumption of dominant heterogeneous nucleation where the temperature dependence of the kinetics is controlled by the linear growth rate. The assumption of heterogeneous nucleation leads to the plot

$$\log (t_{1/2}) + U^*/2.3R(T - T_\infty) \text{ versus } 1/T(\Delta T)f$$

It has been found previously that the actual values used for U^* and T_∞ are of little significance in the kinetic analysis of polyethylene.[16,27] Figures 5 and 6 are close to linear and certainly much more linear than those of Figures 3 and 4, thus confirming the validity of the assumption of predominantly heterogeneous nucleation.

Figures 5 and 6 each contain the kinetic analysis for OPE as a line of reference, since the behavior is well understood. The regime I–regime II transition can be seen to be present at a crystallization temperature corresponding to 123 °C. Above this break, that is at low supercool-

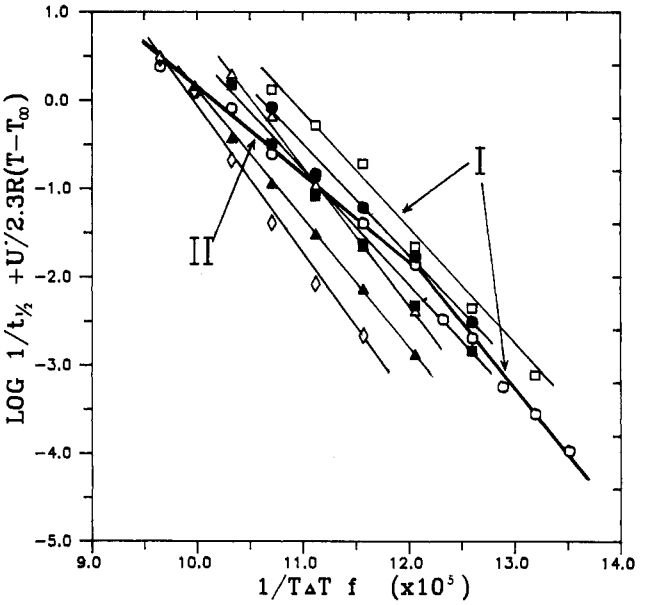

Figure 5. Kinetic behavior of sol fractions assuming heterogeneous nucleation (symbols as in Figure 1).

ings, is found regime I growth (axialites), and below it is regime II growth (spherulites). The growth of axialites and spherulites was confirmed through optical microscopy in the corresponding temperature ranges.

Assignment of the growth regimes for the sol fractions in Figure 5 was made by comparison between the slopes of the sol fractions with those of the well-understood OPE. With use of this method, it can be seen that the slopes of the sol fractions are similar to but not identical with that of OPE in regime I, meaning that growth probably occurs in regime I. Hoffman et al.[2] reported regime I growth for linear PE fractions with weight-average molecular weights ranging from 3600 to 18000, with the growth morphologies being axialitic. The growth of axialites in the sol fractions was observed in this work also, thus supporting the assignment of regime I for the sol fractions, even though the molecules are somewhat branched. It should be recognized that the slopes of the sol fraction curves would not be expected to be identical with that of regime I in OPE since the data are bulk growth rate

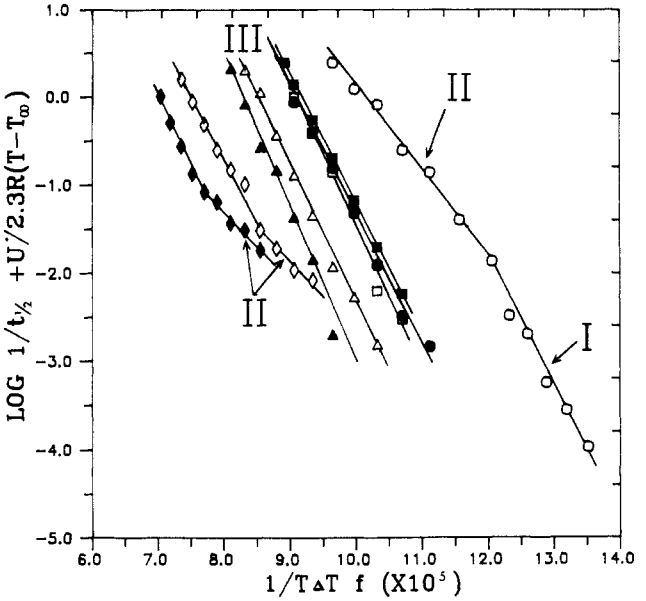

Figure 6. Kinetic behavior of gel fractions assuming heterogeneous nucleation (symbols as in Figure 2).

data and not linear growth rates. Discrepancies might be expected on the basis of differences in nucleation patterns as well as due to potential changes in surface free energy, among several possibilities.

The introduction of cross-links into linear polyethylene alters the crystallization process drastically, as seen in Figure 6. The Lauritzen–Hoffman secondary nucleation theory[1,4] predicts the slopes of regimes I and III to be the same. A comparison of the slopes of the gel fractions with the slope of OPE in regime I indicates that growth occurs primarily in regime III in the gel fractions. The switch from regimes I and II in OPE to regime III in the gel fractions is due to the cross-links reducing the rate of lateral spreading by eliminating the ability of the chains to reptate. Reptation of the cross-linked chains cannot occur since they have no free chain ends. A major reduction in the lateral growth rate would make the rate of secondary nucleation dominant, thus switching the growth from regimes I and II to regime III.

The regime II–regime III transition in the gel fractions first appears in G-2.5 (molecular weight between cross-links of 1900) at 113 °C and also in G-3.1 (molecular weight between cross-links of 1300) at 109 °C, indicating that the transition temperature is dependent of the cross-link density. The reappearance of regime II in the highest cross-linked systems was not anticipated following the observation of only regime III for the lower level cross-linked systems. In the preceding analyses, the equilibrium melting point has been assumed to be that of linear polyethylene. This assumption is reasonable if the cross-links are all excluded from the crystal and do not significantly effect the thermodynamics of the noncrystalline state. The supercoolings corresponding to the regime II–regime III transitions are calculated to be 31.3 K for G-2.5 and 35.3 K for G-3.1. It is possible that the cross-links are included in the crystals at low levels and that the supercoolings used include small errors. Conventional T_m versus T_c plots were close to horizontal for the gels, and equilibrium melting points could not be obtained. Studies are in hand to determine the long periods, and hence lamellar thicknesses, using small-angle X-ray scattering, which should permit resolution of this point of uncertainty.

In the analysis of bulk growth rates it is not expected that the ratios of the slopes of any two regime regions,

Table III
Slopes of Secondary Nucleation Plots

sample	slope from regime analysis, $\times 10^{-5}$ K^2		ratio of slopes I/II or III/II
	sol	gel	
OPE	1.40 (I) 0.94 (II)	...	1.49
0.1	1.22	1.42	
0.3	1.35	1.61	
0.5	1.32	1.47	
0.9	1.44	1.60	
1.2	1.44	1.88	
1.8	...	1.48	
2.5	1.71	0.74 (II) 1.42 (III)	1.92
3.1	...	0.78 (II) 1.78 (III)	2.28

such as those in Figures 5 and 6, should equal the theoretical values of 2. In the analysis of linear growth rates, values close to 2 can be obtained in fractions,[2,6] although in unfractionated samples a value less than 2 is common.[5] Because of the complex nature of the bulk growth process, minor changes in slope might be expected as chain microstructure is changed progressively in a series such as that being considered here. Nevertheless, it is instructive to list the values of the slopes obtained and to calculate the slope ratios whenever two regimes occur. This has been done for the specimens of this study, and data are presented in Table III. It can be seen that the slope ratio of regime I to regime II for OPE is much less than 2; however, the ratios of regime III to regime II in the gel fractions are close to 2. When the sol and gel series are considered separately, the following trends emerge. For the sol series, the slopes are generally slightly lower than that of regime I in OPE. There may be an indication of a general trend downwards with increasing cross-linking agent concentration. In the case of the gel series, the regime III slopes are remarkably close to that of regime I in OPE, whereas the regime II slope is close to that of OPE only for G-2.5.

It is known, however, that the presence of foreign microstructural units, in the form of a comonomer or a defect, reduces the rate of linear growth of a lamella. This effect is a result of the necessity for the rejection of the foreign unit from the crystal nucleus reducing the rate of formation of secondary nuclei. For the cross-linked systems studied here, the presence of sufficient cross-links to generate a gel eliminates the normal method of chain motion through reptation. As mentioned earlier, this results in a major reduction in the rate of substrate completion, which is largely determined by an adjacent reentry process. The rate of secondary nucleation then dominates generating regime III. As cross-link density increases, the remaining modes of chain motion[10–13] are not significantly reduced; however, the rate of secondary nucleation is reduced in a way that produces an inverse logarithmic dependence of nucleation rate on the mole fraction of impurity units.[17] It can therefore be predicted that as impurity unit (i.e. cross-link) concentration increases, the rate of secondary nucleation will decrease until it approaches the rate of substrate completion. At this point regime II reappears, as observed experimentally. Andrews et al.[17] and Rensch et al.[29] have studied the kinetics of crystallization of polymer chains containing imperfections. They found that for a polymer chain with imperfections, there may be sections of chain containing an insufficient number of crystallizable units in sequence to form a critical nucleus, resulting in a reduction in the probability of secondary nucleation. Andrews

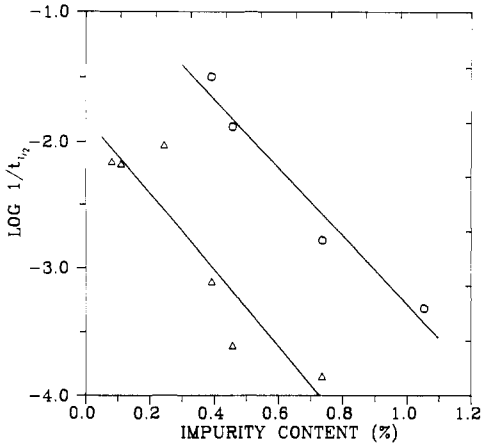

Figure 7. log of reciprocal halftime versus impurity content for gel fractions crystallized as 112 and 116 °C (○, -112 °C; △, -116 °C).

et al.[17] derived an expression for the dependence of the rate of linear growth on impurity content and applied it to explain the effect of trans content at a given temperature on hevea rubber (*cis*-polyisoprene). Similar studies using partially oxidized *cis*-polyisoprene (guayule rubber) showed the behavior to be general and independent of the chemical form of the rejected impurity.[29] This expression is

$$\ln G \simeq -(N-1)\beta + \ln G_0$$

where G is the growth rate, N the minimum number of crystallizable units in sequence required to form a secondary nucleus, β the fractional content of foreign units, and G_0 the growth rate of a pure homopolymer. This approach will now be applied to the data on cross-linked linear polyethylene. With use of the reciprocal halftimes at 112 and 116 °C in place of the growth rate, it can be seen in Figure 7 that the analysis of Andrews et al. does apply to the gel systems where the points used were taken only from regime III. This being the case, then at higher crystallization temperatures, the rate of nucleation would be expected to decrease and become of similar magnitude to the rate of strip growth, making the reappearance of regime II possible. Although there is considerable scatter in the data, straight line fits have been applied since, at this stage, there is no reason to assume a more complicated fit. Of concern in Figure 7 is the initial upswing in the plotted data at low impurity content for the 116 °C curve, this also being reflected in the kinetic data in Figures 2 and 6. The reason for this behavior is unclear at this time, although lamellar thickness data may provide insight into this effect. If a limited number of cross-links were to be incorporated into the crystals, higher lamellar thicknesses would be expected[30] which could result in an increased crystallinity, thus causing the upswing. The needed experiments are currently in progress.

Further analysis of Figure 7 raises a rather interesting point. It is possible to calculate the size of a critical nucleus, that is the minimum number of crystallizable units in sequence, N, required to participate in the formation of a secondary nucleus from the slopes of these plots. The calculated values for N are 269 and 301 for 112 and 116 °C, respectively, and would correspond to methylene units. Assuming a typical lamellar thickness for polyethylene of 120–150 Å, it can be seen from the calculated values of N that the critical nucleus consists of three stems in the case of cross-linked polyethylene.

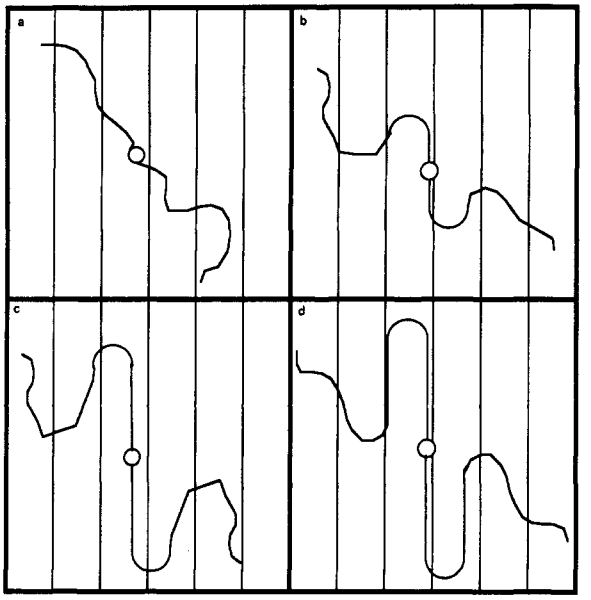

Figure 8. Schematic diagram of the three stem nucleus.

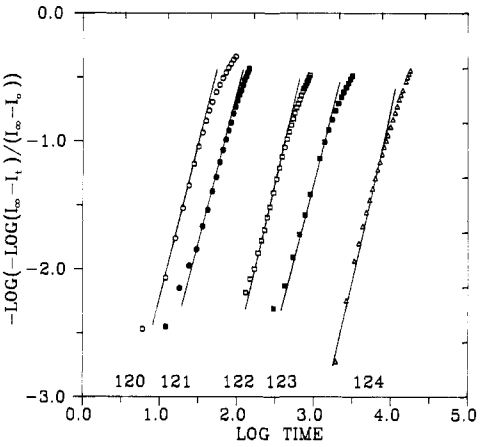

Figure 9. Avrami plot of S-0.1 (M_n = 7106).

Andrews et al.[17] concluded that a three-stem nucleus was present in the case of *cis*-polyisoprene.

The theories of secondary nucleation of Hoffman et al.[1,4,15,23] all assume initial attachment of a polymer chain to the crystal through the chain end. This is because the entropy drop is significantly lower for chain end attachment than for center chain attachment. In the case of a cross-linked polymer, this cannot occur except for chains that might be present as long branches. For chain end attachment the critical nucleus is one stem long, unlike the three-stem nucleus found to be present here, using the Andrews analysis. The reason can be simply envisioned as depicted in Figure 8. A section of the central chain that straightens on the crystal substrate must naturally form two constricted loops that could develop into two adjacent reentry folds and generate a nucleus composed of one complete stem, two half stems, and the two folds. Apparently a similar situation occurs in natural rubber, a high molecular weight polymer where the chains are sufficiently long to be above the entanglement limit. It is possible that entanglements are serving as virtual cross-links, although it is also likely that the molecule nucleates on several lamellae concurrently[31] because of its large size. For the latter situation all but the two nuclei generated from the ends must be of the three-stem variety.

This new information, although in conflict with the single stem model, need not be at variance with regime

Table IV
Avrami Coefficients of Sol Fractions

cryst temp, °C	sample						
	OPE	S-0.1	S-0.3	S-0.5	S-0.9	S-1.2	S-2.5
117	3.1						2.7
118	2.9					2.2	2.0
119	2.9			3.1	2.7	2.2	2.3
120	2.8	2.4	2.7	2.8	2.2	2.8	2.4
121	3.0	2.2	2.8	2.5	2.7	2.0	2.9
122	3.0	2.4	2.5	2.3	2.8	2.0	1.6
123	2.7	2.2	2.6	2.5	3.5	1.6	
124	3.0	2.4	2.4	2.0	3.6		
125			2.5				

Table V
Avrami Coefficients of Gel Fractions

cryst temp, °C	sample						
	G-0.1	G-0.3	G-0.5	G-0.9	G-1.2	G-2.5	G-3.1
105							1.8
106							1.9
107						2.0	1.2
108						2.1	1.8
109						2.1	1.5
110						2.1	1.2
111					2.4	2.0	1.2
112				2.0	2.2	1.9	1.3
113				2.7	2.1	1.9	
114		2.0		2.3	2.3	1.9	1.1
115	2.5	2.2	2.4	2.0	2.2	2.0	
116	2.4	2.0	2.2	2.1	2.2	1.7	
117	2.1	2.2	2.5	2.2			
118	2.2	2.4	2.3	1.7			
119	2.6	2.3	2.6	1.7			
120	2.7	2.4	2.5				
121	2.3						

analyses. Just as the single stem model is only one way of looking at the generally accepted phenomenon of secondary nucleation, so also are regime transitions a general phenomenon. They depend only on the relative rates of secondary nucleation and substrate completion. It should be recognized that the general phenomenology of regimes is independent of the detailed model of initial chain attachment. Clearly, however, it is necessary for another version of secondary nucleation theory to be derived for the three stem nucleus in order for more substantial analyses of these data to be made.

The Avrami analysis may be used to gain some additional insight into the crystallization kinetics of the sol and gel fractions. This is carried out by plotting log $(-\log (I_\infty - I_t)/(I_\infty - I_0))$ versus log time. The Avrami coefficients were obtained as the slopes of the linear regions of such plots. While the number of Avrami plots is too numerous to present, typical examples for the sol and gel fractions are given in Figures 9 and 10, respectively. The Avrami coefficients obtained may be seen in Tables IV and V.

Avrami coefficients for the sol fractions which are given in Table IV, typically average about 2.5, although values in some cases are far above and below this average. Fractional values of Avrami coefficients are not unusual, but values between 2 and 3 are not common. Such a value is intermediate between the theoretically derived values for heterogeneously nucleated disks and spheres. There are no theoretical values available for the Avrami coefficient of an axialite, and so there is some intrinsic interest in what such a value might be. The structure of an axialite may be considered intermediate between the structures of a disk and a sphere, so that a value of 2.5 for the sol fractions is consistent with the presence of axialites observed through optical microscopy.

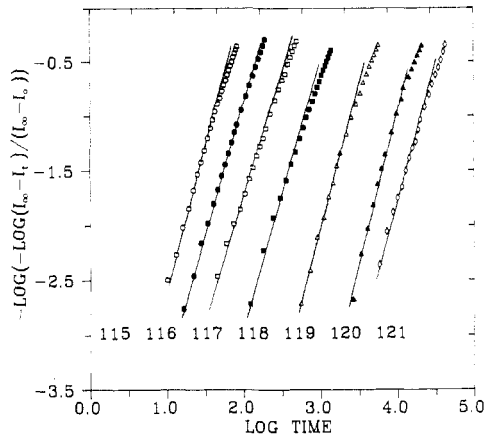

Figure 10. Avrami plot of G-0.1 (molecular weight between cross-links of 17 300).

The Avrami coefficients of the gel fractions range from approximately 2.4 down to 1.3 as can be seen in Table V. Strict interpretation of these values suggests that the morphology of the gel fractions changes from heterogeneously nucleated disks to fibrils or rods. As the cross-link density increases, the Avrami coefficients imply that the gel fractions contain an increasingly large fraction of rodlike entities. This may be caused by an intrinsic change in the growth mechanism or may reflect the presence of row-nucleated species due to frozen-in stress on a microscopic scale in the gel network.

Conclusions

Analysis of the bulk crystallization kinetics of the sol fractions of cross-linked linear polyethylene shows that these low molecular weight fractions follow regime I growth. This conclusion is supported by the observation of axialites through optical microscopy and calculated Avrami coefficients of 2.5. Gel fractions follow regime III growth primarily, with a regime II–regime III transition being observed for the highest cross-link densities. The occurrence of regime III immediately on formation of the gel of least cross-link density suggests that reptation is critical for rapid substrate completion, but not for secondary nucleation. The observation of regime II growth in the cross-linked systems may be explained by a decrease in the rate of secondary nucleation with cross-link density. Data suggest that the critical nucleus of the cross-link systems consists of three adjacently reentered stems.

Acknowledgment. This research has been supported by the Polymers Program of the National Science Foundation under Grants DMR-8608232 and DMR-8719028.

References and Notes

(1) Lauritzen, J.; Hoffman, J. D. *J. Appl. Phys.* **1973**, *44*, 4340.
(2) Hoffman, J. D.; Frolen, L. J.; Ross, G. S.; Lauritzen, J. I. *J. Res. Natl. Bur. Stand., Sect. A* **1975**, *79A*, 671.
(3) Phillips, P. J. *Polym. Prepr.* **1979**, *20*, 438.
(4) Hoffman, J. D. *Polymer* **1983**, *24*, 3.
(5) Lovinger, A. J.; Davis, D. D.; Padden, F. J. *Polymer* **1985**, *26*, 1595.
(6) Phillips, P. J.; Vatansever, N. *Macromolecules* **1987**, *20*, 2138.
(7) Lazcano, S.; Fatou, J. G.; Marco, C.; Bello, A. *Polymer* **1988**, *29*, 2076.
(8) Cheng, S. Z. D.; Janimak, J. J.; Zhang, A.; Cheng, H. N. *Macromolecules* **1990**, *23*, 298.
(9) Cheng, S. Z. D.; Chen, J.; Janimak, J. J. *Polymer*, in press.
(10) Lin, Y. H. *J. Non-Newtonian Fluid Mech.* **1987**, *23*, 163.
(11) Lin, Y. H. *Macromolecules* **1984**, *17*, 2846.
(12) Lin, Y. H. *Macromolecules* **1986**, *19*, 159.
(13) Lin, Y. H. *Macromolecules* **1987**, *20*, 3080.

(14) de Gennes, P. G. *Scaling Concepts in Polymer Physics*, Cornell University Press: Ithaca, NY, 1979.
(15) Hoffman, J. D. *Polymer* **1982**, *23*, 656.
(16) Phillips, P. J.; Kao, Y. H. *Polymer* **1986**, *27*, 1679.
(17) Andrews, E. H.; Owen, P. J.; Singh, A. *Proc. R. Soc. London* **1971**, *A324*, 79.
(18) Lambert, W. S. M.S. Thesis, University of Tennessee, 1988.
(19) Lambert, W. S.; Phillips, P. J., accepted for publication in *Polymer*.
(20) Magill, J. H. *Polymer* **1961**, *2*, 221.
(21) Mayhan, K. G.; James, W. J.; Bosch, W. *J. Appl. Polym. Sci.* **1965**, *9*, 3605.
(22) Phillips, P. J.; Tseng, H. T. *Macromolecules* **1989**, *22*, 1649.
(23) Hoffman, J. D.; Miller, R. L. *Macromolecules* **1988**, *21*, 3038.
(24) Tseng, H. T.; Phillips, P. J. *Macromolecules* **1985**, *18*, 1565.
(25) Ross, G. S.; Frolen, L. J. *J. Res. Natl. Bur. Stand., Sect. A* **1975**, *79A*, 701.
(26) Suzuki, T.; Kovacs, A. J. *Polym. J.* **1970**, *1*, 82.
(27) Davidson, T.; Wunderlich, B. *J. Polym. Sci., Polym. Phys. Ed.* **1969**, *7*, 377.
(28) Boyd, R. H. *Macromolecules* **1984**, *17*, 903.
(29) Rensch, G. J.; Phillips, P. J.; Vatansever, N.; Gonzalez, V. A. *J. Polym. Sci., Polym. Phys. Ed.* **1986**, *24*, 1943.
(30) Sanchez, J. C.; Eby, R. K. *Macromolecules* **1975**, *8*, 638.
(31) Palys, L. H.; Phillips, P. J. *J. Polym. Sci., Polym. Phys. Ed.* **1980**, *18*, 829.

Distribution of Infrared Intensity in the Spectra of Conformationally Disordered Chain Molecule Assemblies

R. G. Snyder

Department of Chemistry, University of California, Berkeley, California 94720.
Received June 16, 1989; Revised Manuscript Received October 16, 1989

ABSTRACT: The distribution of intensity of the infrared spectrum of a simple model system of flexible chain molecules has been examined as a function of conformational disorder in order to establish a basis for the characterization of disorder by vibrational spectroscopy. A finding of practical importance is that the band intensity associated with a delocalized mode is nonlinearly related to the concentration of disorder measured in terms of the conformational state of the bonds and that the degree of the nonlinearity increases with the chain length. Therefore, to determine quantitatively the degree of conformational disorder for an assembly of flexible chain molecules, it is necessary to employ bands associated with modes that are highly localized. A second aspect of this study concerns the well-known observation that, for a given chain molecule system, the degree to which the intensity distribution is affected by a change in the average conformation of the system is dependent on the type of vibrational mode involved. There are two principal factors that determine the sensitivity of an infrared band to conformation. One is the relation, within the repeating unit of the chain, between the direction of the local dipole moment derivative associated with the mode and the direction of the skeletal bond whose internal rotational states determine the conformation of the chain. The second factor concerns how the normal coordinate of the mode is dependent on the conformation of the chain. These two factors are interrelated, and, in fact, depending on the direction of the dipole moment derivative, their effects may cancel. This leads to different modes having different sensitivites to conformational change.

I. Introduction

In this paper we call attention to some general relations between intensity and disorder that bear on the use of infrared and Raman spectroscopy for the determination of conformational disorder in assemblies comprised of chain molecules. These relations are peculiar to the spectra of chain molecules and do not appear to have been previously considered. We will show that the intensities of most infrared and Raman bands in the spectra of chain molecule systems are not linearly related to the degree of conformational disorder if, as is ordinarily the case, the disorder is measured in terms of the concentrations of the various possible conformational states of the skeletal bonds. The departure from linearity may be very large and may therefore lead to correspondingly large systematic errors in the quantitative evaluation of disorder. The nonlinearity is a consequence of the fact that the band intensities used for conformational analysis are associated with modes that are largely delocalized; that is, the normal coordinate of the mode tends to extend over the length of the chain, whereas the conformational statistic that is to be measured, namely, the average conformation of a bond, is a highly localized quantity. On the other hand, we note that a linear relation between intensity and disorder does occur in the less common situation where the band whose intensity is to be used as a measure of disorder is associated with a vibrational mode that is highly localized.

This problem of nonlinearity has been discussed for one particular case by Pink et al.,[1] who recognized that the Raman intensity of the 1130-cm^{-1} C–C stretching band of acyl chains, which is commonly used to estimate conformation disorder in the hydrocarbon component of lipid bilayer membranes, was not, as had been previously assumed, linearly related to chain disorder. These authors used statistical mechanical methods and the results of normal coordinate calculations that had been reported earlier for the C–C stretching modes of hydrocarbon chains[2] to achieve a more accurate calibration. After their results were reported,[1] the high nonlinearity in the relation between the intensity of the 1130-cm^{-1} band and the number of gauche bonds per chain was verified exper-

0024-9297/90/2223-2081$02.50/0